Hostile Area or Facility Monitoring with an Optimal Wireless Sensor Network Deployment

Jenn-Long Liu[#1], Tien-Hui Hsiao[*2]

[#]*Department of Information Management, I-Shou University*
No.1, Sec. 1, Syuecheng Rd., Kaohsiung 840, Taiwan, R.O.C.
[1]jlliu@isu.edu.tw

[*]*Department of Logistics and Marketing management, Leader University*
No 188, Sec. 5, An-Chung Rd., Tainan 709, Taiwan, R.O.C.
[2]sth@mail.leader.edu.tw

***Abstract*— This study uses an enhanced non-dominated sorting genetic algorithm (enhanced MOGA) to generate the optimal wireless sensor network deployment for monitoring a hostile perimeter area or a critical facility. The sensors are deployed around the area for sensing the activities in the area or placed outside the critical facility for sensing the movements of incoming and outgoing of personnel worked in the facility. The distributed sensors are capable of sensing and linking with each other in order to communicate the gathered data via a sensor to a nearby high energy communication node (HECN). The HECN served as a transmission relay to deliver gathered data from the ground to a high-altitude unmanned aerial vehicle (UAV). Two scenarios are implemented by using the enhanced MOGA to achieve the sensor deployment by minimizing the number of sensors and maximizing the coverage. Simulation results will show the Pareto-optimal front, sensor deployment and communication routes between sensors and the HECN.**

***Keywords*— Enhanced multi-objective genetic algorithm, wireless sensor network, critical facility, high energy communication node.**

1. INTRODUCTION

Recently, wireless sensor networks (WSN) play an important role for applying to target detection and mission surveillance. Every type of sensor has its special function, such as for sensing the variations of temperature, sound, humidity, pressure, luminosity or concentration of chemical materials. The sensors not only can detect anything nearby but also can communicate with each other wirelessly. An important issue mentioned in WSN domain is how to achieve an effective surveillance with small-range sensors distributed in the interesting area. Therefore, many researches have shown a raising interest in WSN planning to optimize the location of distributed sensors in order to maximize their sensing region with minimum number of sensors. This manner of planning is almost identical to the base station (BS) placement. A classic example close to the WSN problem is the maximal covering location problem [1], where as many specified points as possible must be covered using some sensors with fixed sensing range. Recently, Chakrabarty *et al.* [2] used an integer linear programming to minimize the total cost of sensors for planning the sensor locations. Also, Zou and Chakrabarty [3] adopted virtual force algorithm (VFA) to improve the coverage of sensor field with constant number of sensors. Only one objective is optimized in their study, it is impossible to obtain the trade-off between number of sensors and coverage. Therefore, a multi-objective algorithm, which can deal with multiple objectives to covering a region with a set of sensors, is desired. Also, particular to WSN involves the relationship between optimal WSN layout and the ratio between the sensing and communication radiuses of sensors [4, 5].

In fact, the applications of WSN are relatively wide, e.g., build up smart environments to life and military operations to surveillance, etc. The smart environment relies on sensory data from the real world in building, utilities, industrial, home, shipboard, and transportation systems automation, and so on. However, the military operations are always applied to place with wireless sensors to monitor the activity or situation on the air or ground. The targets of surveillance include people, facilities or vehicles. Since almost of military missions will be

performed in hostile areas, the placement of such sensors needs to be done with human personal involved, e.g. via aerial deployment from an unmanned aerial vehicle (UAV) as shown in Fig. 1. Once the sensors are deployed on the ground, their sensory data are gathered and transmitted to a high-energy communication node (HECN) or base station in order to provide the transmission relay to an UAV.

Accordingly, this work uses an enhanced multi-objective genetic algorithm (enhanced MOGA) to find Pareto-optimal WSN layouts that maintain the communication connectivity between every sensor and the HECN placed nearby. Two scenario studies are conducted using the enhanced MOGA. In the first one, a specified area, such as a forest perimeter located in the hostile region, is to be uniformly covered by the WSN, so that every point in it can be monitored. The second one, a critical facility is to be monitored by the WSN, so that the movements of personnel worked in the facility can be detected everywhere around the facility. This two scenario studies are basic mission scenarios that can form the primitives of a more complex mission scenario.

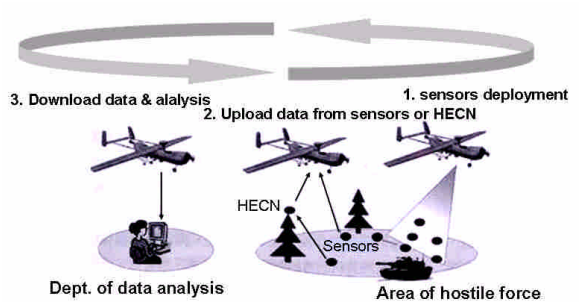

Fig. 1 Processes of sensors deployment, upload data from a HECN to a UAV, and download data from the UAV to home base for data analysis

2. NUMERICAL PROCEDURE

2.1. Multiple Objective Optimization

The general form of a MOOP involves the minimization of objective functions subject to constraints. The mathematical form of the MOOP is

$$\text{Minimize } \vec{f}(\vec{x}) = \{f_1, f_2, ..., f_M\}^T, \quad \vec{x} = \{x_1, x_2, ..., x_n\}^T \tag{1}$$

$$\text{Subject to } g_j(\vec{x}) \geq 0,\ j = 1, ..., p \tag{2}$$

where $\vec{x}$ and $\vec{f}(\vec{x})$ represent the design variable vector and objective function vector in the *n*-dimensional hyperplane with *M* objectives. Also, $g(\vec{x})$ is the constrained function vector with *p* constraints. In a minimization problem, a variable vector $\vec{x}_a$ is said to dominate $\vec{x}_b$ if and only if the following two conditions are satisfied.

$$\forall i \in \{1, 2, ..., M\},\ f_i(\vec{x}_a) \leq f_i(\vec{x}_b) \text{ and}$$
$$\exists j \in \{1, 2, ..., M\},\ f_j(\vec{x}_a) < f_j(\vec{x}_b) \tag{3}$$

Therefore, a feasible solution $\vec{x}^*$ is said to be a Pareto-optimal solution if and only if there does not exist a feasible solution $\vec{x}$ where $\vec{x}$ dominates $\vec{x}^*$, and the corresponding vector of Pareto-optimal solutions forms a so called Pareto-optimal front shown in Fig. 2.

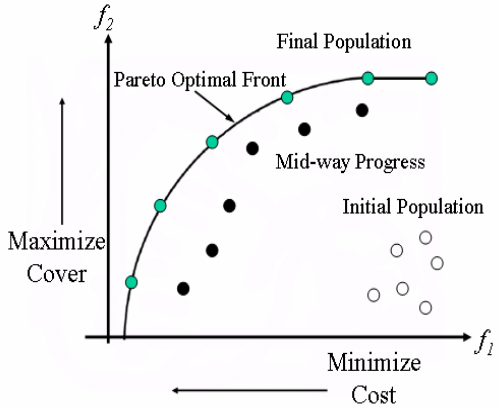

Fig. 2 Dominated solutions, non-dominated solutions and Pareto-optimal front involved in a multi-objective minimization problem

2.2 Flowchart of the Enhanced MOGA

In this study, the enhanced MOGA combines the non-dominated sorting procedure with the elitist strategy, crowding distance sorting, binary tournament selection, extended intermediate crossover and non-uniform mutation. Figure 3 shows the flowchart of the enhanced MOGA. The binary tournament selection operator is based on the crowded-distance comparison. Moreover, the elitist strategy is included in the enhanced MOGA since it improves the performance of evolutionary multi-objective optimization algorithms [6]. The detailed procedures for non-

dominated sorting, binary tournament selection, extended intermediate crossover and non-uniform mutation operators are described in the following Sections 2.3-2.6.

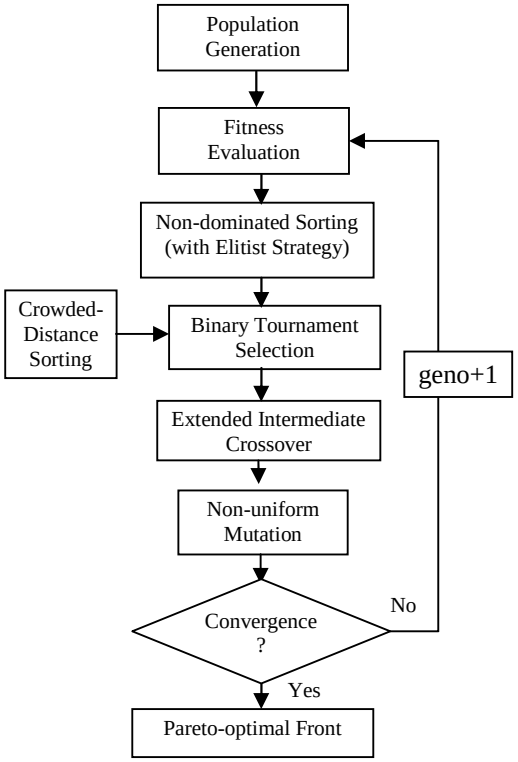

Fig. 3 Flowchart of the enhanced MOGA

2.3 Non-dominated Sorting

The enhanced MOGA first generates a random parent population P_t of size N at generation t=0. The population is then sorted according to the fast non-domination sorting approach [6], in order to assign each solution vector a fitness based on the non-domination ranking level. The best solution has the lowest ranking level. A book-keeping procedure, which uses the information about the set that an individual dominate set (S_p) and the number of individuals that dominate the individual (n_p), is applied to reduce the computational complexity. A child population Q_t of size N at generation t=0 is then created using binary tournament selection (in Section 2.4), extended intermediate crossover (in Section 2.5) and non-uniform mutation (in Section 2.6) operators. Thereafter, the following procedure is applied in each generation. First, the parent and child populations are combined to form a pool population R_t of size $2N$, which is sorted by the fast non-domination sorting approach. Meanwhile, the parent solutions are compared with the child population to ensure elitist strategy. The new parent population is created by adding solutions from the first front and continuing to other fronts successively until the population size exceeds N (Fig. 4). The new parent population with size N is now can be created by computing crowding distance of each individual and using a crowded-comparison operator described in the following Section 2.4.

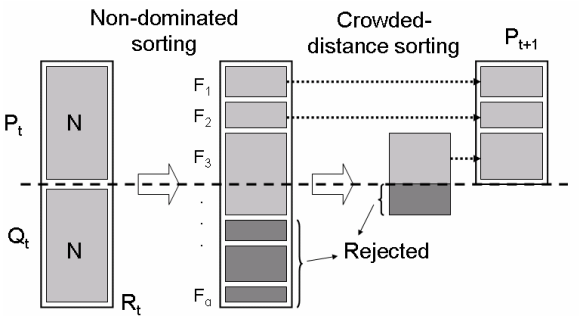

Fig. 4 The procedure of generating individuals with size N via non-dominated sorting and crowded-distance sorting

2.4 Crowded-comparison Operator and Binary Tournament Selection Operator

Once the non-dominated sorting is complete the crowding distance is assigned. The crowding distance for each individual, $i_{distance}$, is computed from the summation of the Euclidean distance between neighbors (i-1) and (i+1) based on sorted fitness values of each objective function [6]. Thereafter, the crowded-comparison operator, $\geq_n$, is employed to ensure the diversity of the last accepted front. The definition $i \geq_n j$ means ($i_{rank}<j_{rank}$) or (($i_{rank=}j_{rank}$) & ($i_{distance}>j_{distance}$)). Namely, the selection is biased towards selecting the solution with the lower rank or larger crowding distance when both points i and j are located on the same front. Consequently, the binary tournament selection operator selects two individuals and selects the best one as the new individual via the crowded-comparison operator. This process is repeated population size of times. Thus, this selection procedure builds the population P_{t+1} with size N as shown in Fig. 4.

2.5 Extended Intermediate Crossover Operator

In the real-coded genetic algorithms, the effect of crossover is corresponding to make the individuals of one pair of parents to get closer or

pull away from each other. This study adopts an extended intermediate crossover (generally named recombination in real-valued genetic algorithm) to fulfill the crossover operator of the enhanced MOGA. The variable vector of offspring ($\vec{x}_c$) is generated by combining two variable vectors of parents ($\vec{x}_{p1}$ and $\vec{x}_{p2}$), as listed below [7].

$$\vec{x}_c = \vec{x}_{p1} + \alpha(\vec{x}_{p2} - \vec{x}_{p1}) \quad (4)$$

The parameter α is a scaling factor chosen uniformly at random over an interval [$-d$, 1 + d] with d=0.25 being a good of parameter value. Each variable of $\vec{x}_c$ is the result of combining the variables according to the above expression with a new α chosen for each variable.

2.6 Non-uniform Mutation Operator

A non-uniform mutation operator [8] is then applied after the crossover operator is completed to enhance the fine-turning capabilities of the enhanced MOGA. For a parent $\vec{x}$ with n variables $[x_1,...,x_l,...,x_n]$, if the variable $x_l \in [u_l, l_l]$ is selected for the non-uniform mutation, then the variables of parent are exchanged to $\vec{x}' = [x_1,...,x_l^{'},...,x_n]$. The variable x_l' , which is the one of the variables $\vec{x}'$, is derived as follows.

$$x_l^{'} = \begin{cases} x_l + \Delta(t, u_l - x_l), \text{if } 0 \le r < 0.5 \\ x_l - \Delta(t, x_l - l_l), \text{if } 0.5 \le r \le 1 \end{cases} \quad (5)$$

The terms t and r represent the generation number and a random number in the range [0, 1], respectively. The function $\Delta(t, y)$ is expressed as

$$\Delta(t, y) = y(1 - r^{(1-t/T)^b}) \quad (6)$$

where T is the maximal number of generation, and b is a user-specified parameter for controlling the degree of non-uniformity. This study set b=0.1 that results in a good performance for the enhanced MOGA. It is noted that the value of the function $\Delta(t, y)$ is located in the range [0, y] as shown in Fig. 5. Figure 5 also shows the non-uniform mutation produces the individuals to search space uniformly at former stages when the number of generation t is small, and locally when the number of generation t approaches to T.

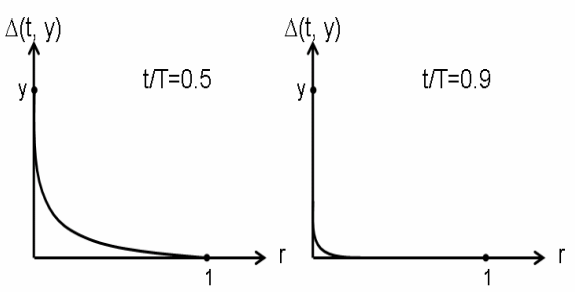

Fig. 5 Mutations at t/T=0.5 and t/T=0.9 time steps using the function Δ(t, y)

3. RESULTS AND DISCUSSIONS

To handle mobile base station placement problems, the representation of an individual in the enhanced MOGA is denoted as a vector $(c_1,..., c_n, b_1,..., b_n)$ where $c_i=(x_i, y_i)$ denotes the i-th base station position; b_i=0 or 1 is the active Boolean logic value of the i-th base station to enable or disable the base station. The fitness functions are specified as the total number of sensors (f_1) and total coverage (f_2).

3.1 Scenario 1: Motoring an Area by the WSN

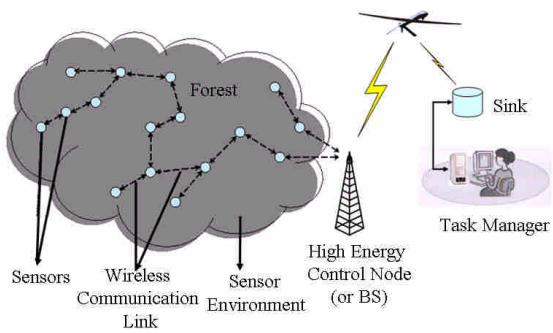

Fig. 6 Scenario of uniformly monitoring an area by the WSN

Figure 6 displays the scenario that an area, such as forest in the hostile region, is monitored by the WSN. Sensors are distributed uniformly to cover the region. Sensors are capable of communicating with each other to transmit information to HECN and the HECN is able to provide the transmission relay to a UAV. To simulate this scenario, this work simplifies the monitored area as an elliptic

domain within a 10×10 domain. The lengths of semi-major axis and semi-minor axis were 4.0 and 3.0, respectively. The HECN is located at the point (5.0, 5.0). Also, the maximum number of sensors and ratio of sensing and communication radiuses were 20 and 1.4/3.0, respectively. Twenty repeated runs are implemented for the simulation. Two objective functions are applied to minimize the number of sensors and to maximize the coverage. The expression of the two objective functions is expressed as follows.

$$\text{Minimize } f_1(\vec{x}) = \sum_{i=1}^{n} b_i \tag{7}$$

$$\text{Maxmize } f_2(\vec{x}) = \frac{\sum_{i=1}^{n} \cup \left[\pi r_{sensing}^2(x_i, y_i) \times b_i\right]}{\text{Area}} \tag{8}$$

where the symbol $r_{sensing}$ represents the sensing radius of a sensor located at (x_i, y_i) and Area denotes the interesting area of monitoring. Figure 7 shows the Pareto-optimal front of scenario 1 with maximum coverage close to 100% when using 9 sensors to cover the ellipse. To further understand the coverage and distribution of sensors, Figures 8(a)-(d) show the sensing and communication distributions of 6, 9, 12 and 15 sensors, respectively. The sensors should to cover the elliptic area (inside the boldface black line), communicate with each other, and at least one sensor should be communicated with the HECN. The ranges of sensing and communication of each sensor are marked as blue solid and red dash lines, respectively, and the communicated routes are connected by the thin black lines. Figures 8(a)-(d) show that the connectivity for each sensor to other sensors holds. Table 1 lists the detailed results of number of sensors versus coverage after 20 repeated runs.

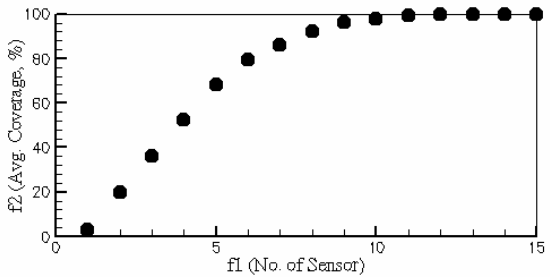

Fig. 7 Pareto-optimal front of scenario 1

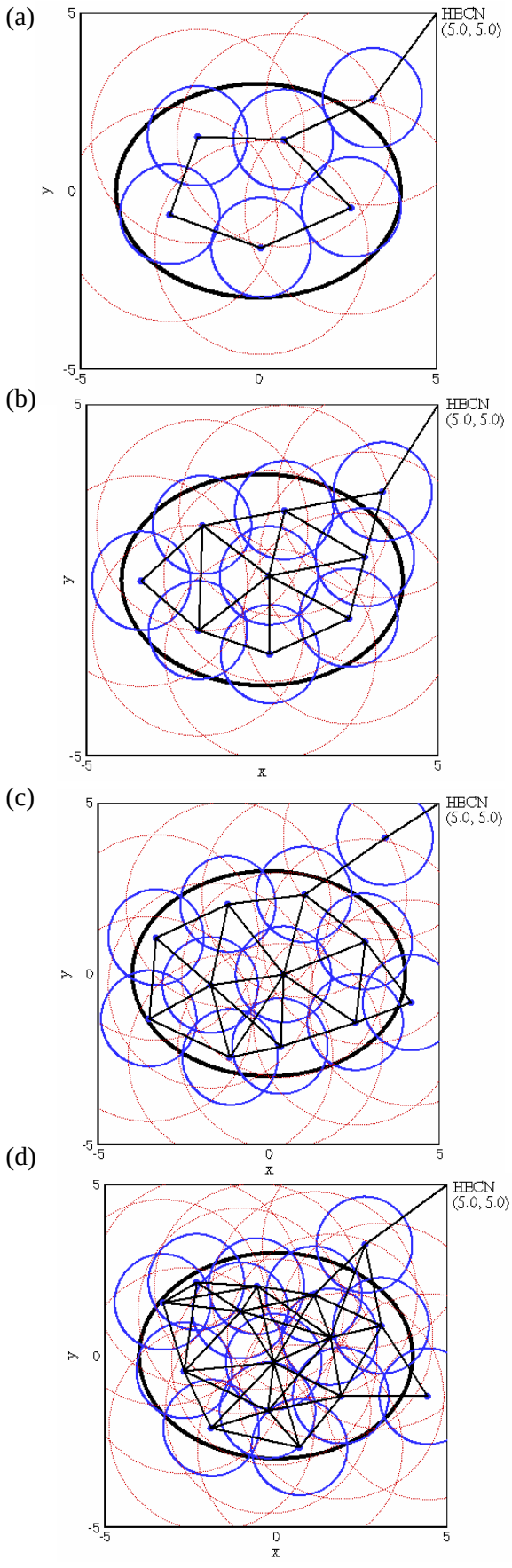

Fig. 8 Distributions of sensing and communication using (a) 6, (b) 9, (c) 12 and (d) 15 sensors for scenario 1

3.2 Scenario 2: Motoring a Hostile Facility by the WSN

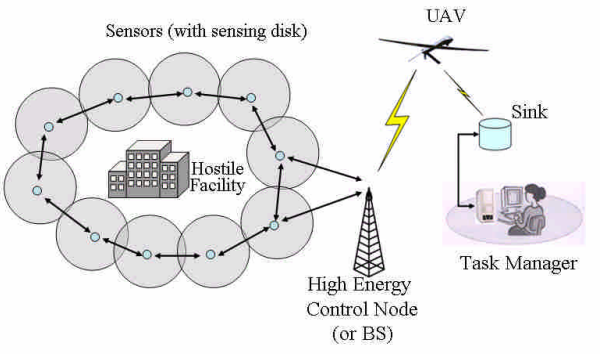

Fig. 9 Scenario of monitoring a hostile facility by the WSN

Figure 9 displays the scenario that a hostile facility is monitored by the WSN. Sensors are distributed around outside the facility to detect the movements in and out the facility. Sensors are also capable of communicating with each other to transmit gathered information to the HECN which is able to provide the transmission relay to a UAV. To simulate this scenario, this study uses the entire interesting region as a 10×10 square domain. The position of HECN is located at the point (5.0, 5.0). Also, the maximum number of sensors and ratio of sensing and communication radiuses were 20 and 1.4/3.0, respectively. Two geometries of monitored facility are studied. The one is a circular facility and another is a hexagon one. Two objective functions are implemented using the enhanced MOGA. The first objective function is to minimize the number of sensors, and the second one is to maximize the coverage. Lines are generated around the circle or hexagon. Thus, the expression of the two objective functions is expressed as follows.

$$\text{Minimize } f_1(\vec{x}) = \sum_{i=1}^{n} b_i \qquad (9)$$

$$\text{Maxmize } f_2(\vec{x}) = \frac{\text{Lines covered}}{\text{Total number of lines}} \qquad (10)$$

3.2.1 Circular Facility Monitoring

In the first case of monitoring the hostile facility, the geometry of facility is simplified to a circle. The sensors should be placed outside the circular perimeter and can be communicated with each other. Figure 10 depicts the Pareto-optimal front with average coverage 99.28% when using 11 sensors to monitor the perimeter. Figure 11 displays the best distributions of sensing and communication with 10 sensors. The communication between each sensor is complete. Also, the sensor nearby HECN is linkable to transmit the gathered sensing data of sensors to the HECN in order to perform the transmission relay to a UAV. TABLE 2 lists the detailed results of number of sensors versus coverage after 20 repeated runs.

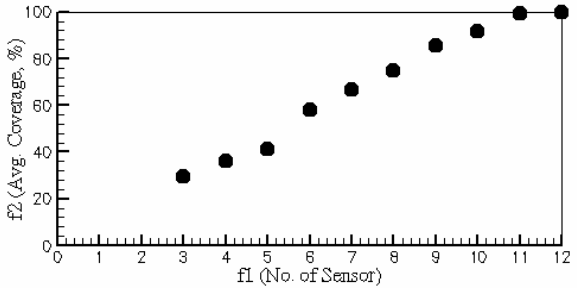

Fig. 10 Pareto-optimal front of scenario 2 on monitoring the circular facility

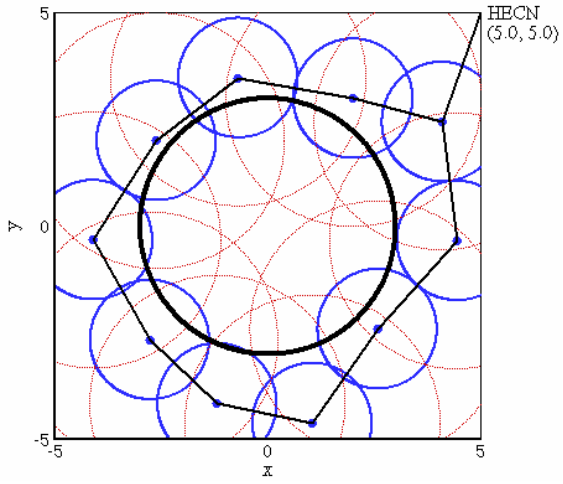

Fig. 11 Distributions of sensing and communication with 10 sensors of scenario 2 on monitoring the circular facility

3.2.2 Hexagon Facility Monitoring

The second case of monitoring the hostile facility is to assume the geometry of the hostile facility is a hexagon. Also, the sensors should be placed outside the hexagon facility and can be communicated with each other. It is noted that this case is more difficult than the former case shown in Sec. 3.2.1 because of the constrained setting of sensors which need to be checked whether the positions are located outside the

hexagon facility. This study first divided the hexagon facility to six equilateral triangles and then verified the position of sensor located inside or outside the triangles. If the position of a sensor located in any one triangle, we set the constraint as a negative value, otherwise give a positive value. Figure 12 shows the result of the Pareto-optimal front which the coverage almost reaches 100% when using 10 sensors to monitor the hexagon perimeter. Figure 13 displays the best distributions of sensing and communication with 9 sensors. The communication between any sensors is complete. Also, a sensor nearby the HECN is linkable to transmit sensing data of all sensors to the HECN in order to fulfill the transmission relay to a UAV. TABLE 3 lists the detailed results of number of sensors versus coverage after 20 repeated runs.

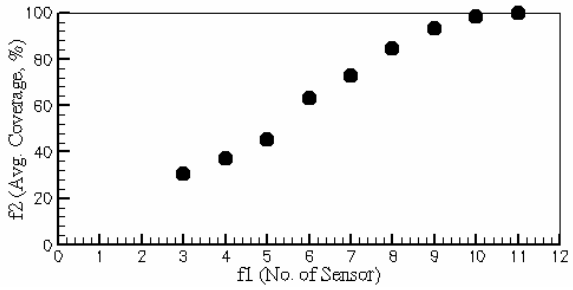

Fig. 12 Pareto-optimal front of scenario 2 on monitoring the hexagon facility

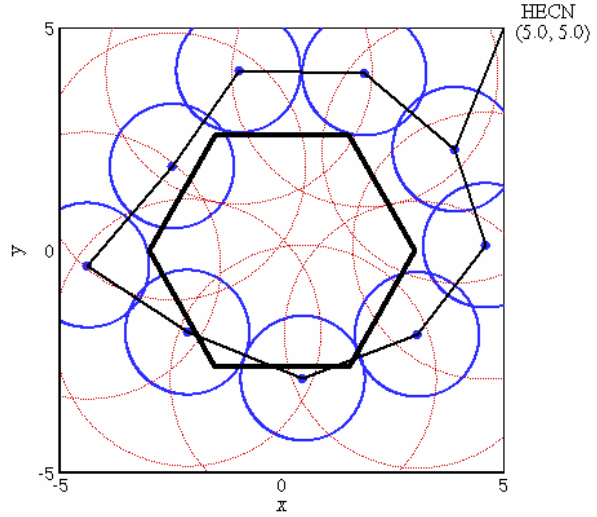

Fig. 13 Distributions of sensing and communication with 9 sensors of scenario 2 on monitoring the hexagon facility

4. CONCLUSIONS

The study has applied the enhanced MOGA, which combines the non-dominated sorting procedure with elitist strategy, crowded distance sorting, tournament selection, extended intermediate crossover and non-uniform mutation operators, to solve the monitoring problems of WSN deployment. Two scenarios of monitoring problems are studied. The first one is to deploy sensors in an elliptic area in order to monitor the activities within the area. Results show that sensors are linkable each other and able to communicate with the nearby HECN for further transmission relay for gathered data to a UAV. The best maximum coverage reaches 100% when using 13 sensors to monitor the elliptic perimeter area. The second scenario was to deploy sensors around a circle and hexagon facilities to monitor the movements of incoming and outgoing of personnel worked in the facility. Simulation results show that the best maximum coverage reaches 100% when using 10 and 9 sensors deployed around a circle and hexagon facilities.

REFERENCES

[1] A. Mehzer, A. Stulman, "The maximal covering location problem with facility placement on the entire plane," *Journal of Regional Science*, vol. 22, no. 3, 1982.

[2] K. Chakrabarty, S. S. Iyengar, H. Qi and E. Cho, "Grid coverage for surveillance and target location in distributed sensor networks," *IEEE Transactions on Computers*, vol. 51, pp. 1448-1453, Dec. 2002.

[3] Y. Zou and K. Chakrabarty, "Sensor deployment and target localization based on virtual forces," *Proc. IEEE Infocom Conference*, vol. 2, pp. 1293-1303, Apr. 2003.

[4] D. B. Jourdan and O. L. de Weck, "Layout optimization for a wireless sensor network using a multi-objective genetic algorithm," in *Proc. IEEE Vehicular Technology Conference*, Milan, May 2004.

[5] D. B. Jourdan and O. L. de Weck. Multi-objective genetic algorithm for the automated planning of a wireless sensor network to monitor a critical facility. In *Proc. SPIE Defense and Security Symposium*, pp 565–575, Orlando, Florida, 2004.

[6] K. Deb, A. Pratap, A. Agarwal, and T. Meyarivan, "A Fast and Elitist Multi-objective Genetic Algorithm: NSGA-II,"

IEEE Trans. on Evolutionary Computation, vol. 6, no. 2, pp. 182-197, Apr. 2002.

[7] H, Mühlenbein and D, Schlierkamp-Voosen, "Predictive Models for the Breeder Genetic Algorithm I - Continuous Parameter Optimization," *Evolutionary Computation*, vol. 1, no. 1, pp. 25-49, 1993.

[8] M.M. Raghuwanshi, O.G. Kakde, "Survey on multiobjective evolutionary and real coded genetic algorithms," in *8th Asia Pacific Symposium on Intelligent and Evolutionary Systems*, Cairns, Australia, pp. 150-161, 2004.

TABLE 1
RESULTS OF NUMBER OF SENSORS VERSUS COVERAGE (MONITORING FOR AN ELLIPTIC AREA)

number of sensor	average coverage	maximum coverage	minimum coverage	standard deviation
1	3.118179%	3.353737%	2.395531%	0.002517
2	19.610062%	19.882889%	18.898056%	0.002546
3	36.108593%	36.358795%	35.373970%	0.002669
4	52.335640%	52.861324%	51.370773%	0.004171
5	68.102211%	69.177536%	66.648926%	0.007151
6	79.311951%	80.889008%	77.535263%	0.010067
7	86.080650%	88.155441%	84.216133%	0.010193
8	92.197235%	94.357201%	90.284798%	0.010917
9	96.330849%	97.551239%	95.102478%	0.006991
10	97.982430%	98.749001%	96.859200%	0.005869
11	99.079613%	99.760445%	97.870644%	0.004196
12	99.625961%	99.946770%	98.882088%	0.002378
13	99.850105%	100.000000%	99.494278%	0.001479
14	99.925476%	100.00000%	99.760445%	0.000779
15	99.926804%	100.00000%	99.787064%	0.000828

TABLE 2
RESULTS OF NUMBER OF SENSORS VERSUS COVERAGE (MONITORING FOR A CIRCLE FACILITY)

number of sensor	average coverage	maximum coverage	minimum coverage	standard deviation
3	29.682541%	31.111115%	27.222221%	0.012192
4	36.269840%	39.722221%	32.777779%	0.022016
5	41.190472%	44.444443%	38.055557%	0.024385
6	58.194443%	62.222221%	51.388889%	0.030283
7	66.708336%	71.666664%	59.722221%	0.032302
8	74.907410%	81.666664%	67.222221%	0.039253
9	85.774857%	100.000000%	72.222221%	0.092544
10	91.503265%	100.000000%	79.722221%	0.082325
11	99.277779%	100.000000%	93.611115%	0.019052
12	100.000000%	100.000000%	100.000000%	0.000000

TABLE 3
RESULTS OF NUMBER OF SENSORS VERSUS COVERAGE (MONITORING FOR A HEXAGON FACILITY)

number of sensor	average coverage	maximum coverage	minimum coverage	standard deviation
3	30.580811%	36.944443%	18.333336%	0.051335
4	37.098770%	41.388889%	30.277779%	0.034424
5	45.166668%	52.777779%	35.555557%	0.056835
6	63.069447%	70.277779%	55.833332%	0.041262
7	72.680557%	81.388885%	64.722221%	0.047736
8	84.777779%	100.00000%	72.222221%	0.089368
9	93.296295%	100.00000%	77.777779%	0.076879
10	98.425926%	100.00000%	91.111115%	0.030654
11	100.00000%	100.00000%	100.00000%	0.000000